33ND INTERNATIONAL COSMIC RAY CONFERENCE, RIO DE JANEIRO 2013
THE ASTROPARTICLE PHYSICS CONFERENCE

Cosmic-ray muon flux at very high energies

T. S. SINEGOVSKAYA[1], A. A. KOCHANOV[2], S. I. SINEGOVSKY[3]

[1] *Department of Higher Mathematics, Irkutsk State Railway U., 664074 Irkutsk, Russia*
[2] *Institute of SolarTerrestrial Physics, Russian Academy of Sciences, Irkutsk, 664033 Russia*
[3] *Institute of Applied Physics, Irkutsk State U., 664003 Irkutsk, Russia*

sinegovsky@api.isu.ru

Abstract: The atmospheric muon fluxes at different zenith angles are calculated in the energy region above 1 TeV with usage of known hadronic models QGSJET-II-03, SIBYLL 2.1, and also the model by Kimel and Mokhov. The computation of the muon fluxes is made with a method to solve the hadronnucleus cascade equations for the non-power primary cosmic ray spectra taking into account a violation of the Feynman scaling of inclusive cross sections and the growth with energy of inelastic cross sections for hadronnucleus collisions. The calculations are performed for a wide class of hadron-nucleus interaction models using directly the primary spectra obtained in the ATIC-2, KADCADE and GAMMA experiments as well as the parameterisations of the primary spectrum based on a set of experiments. Comparison of the calculated muon energy spectra at sea level with the data from a number of experiments shows that hadronnucleus interactions are a source of appreciable uncertainty in the energy region beyond the the knee in the primary spectrum. The prompt muon flux due to decays of the charmed hadrons is reanalysed. Seemingly the prompt muon flux higher than one predicted with usage of QGSM is excluded by the IceCube measurements of the atmospheric neutrino flux. One may hope that more strong restriction of the prompt muon flux range will be extracted from the experiment in the near future.

Keywords: cosmic rays, atmospheric muons, high-energy hadronic interactions

1 Introduction

Measurements of the spectrum and zenith-angle distribution of high- and ultrahigh-energy cosmic ray muons make possible an extraction of characteristics of hadron-nucleus interactions in case the spectra of primary cosmic rays are well known. Comparison of the calculations with the EAS component measurements could give information about the details of the interactions that manifest themselves in the measured characteristics of the secondary cosmic ray fluxes.

The atmospheric muon flux as well as muon neutrino flux at high energies are inevitably dominated by the prompt component due to decays of the charmed hadrons ($D^{\pm}$, D^0, $\overline{D}^0$, $D_s^{\pm}$, Λ_c^+), hence the prompt neutrino flux becomes the major source of the background in the search for a diffuse astrophysical neutrino flux. Insufficiently explored processes of the charm production give rise to most uncertainty in the muon and neutrino fluxes. Besides, an ambiguity in high-energy behaviour of pion and kaon production cross sections affects essentially the atmospheric muon and neutrino fluxes. Recent calculations[1, 2] reveal differences (up to factor 1.5 at 10 PeV) in the neutrino flux because of uncertain description of the hadronic proceses involving light quarks at high energies.

In this work we extend to higher energies the conventional muon flux calculations basing on the known hadronic interaction models with usage reliable data of the primary cosmic ray measurements. We present results of the conventional muon flux calculations in the energy range 10^5–10^8 GeV using hadronic models QGSJET-II [3], SIBYLL 2.1 [4] and the model by Kimel and Mokhov (KM) [5], that were tested also the atmospheric muon flux calculations[6, 7]. In order to compare the uncetainty of the conventional muon flux and prompt one we plot the prompt muon contrubition originating from decays of the charmed hadrons produced in collisions of cosmic rays with nuclei of air.

2 The method of calculations

The high-energy muon fluxes are calculated using the method [6, 8] to solve hadronic cascade equations in the general case of non-scaling behavior of the particle production cross-sections, the rise of total inelastic hadron-nuclei cross-sections, and the non-power law primary spectrum is considered. To obtain the differential energy spectra of protons $p(E,h)$ and neutrons $n(E,h)$ at the depth h one needs to solve the set of equations:

$$\frac{\partial N^{\pm}(E,h)}{\partial h} = -\frac{N^{\pm}(E,h)}{\lambda_N(E)} + \\ + \frac{1}{\lambda_N(E)} \int_0^1 \Phi_{NN}^{\pm}(E,x) N^{\pm}(E/x,h) \frac{dx}{x^2}, \quad (1)$$

where $N^{\pm}(E,h) = p(E,h) \pm n(E,h)$,

$$\Phi_{NN}^{\pm}(E,x) = \frac{E}{\sigma_{pA}^{in}(E)} \left[\frac{d\sigma_{pp}(E_0,E)}{dE} \pm \frac{d\sigma_{pn}(E_0,E)}{dE} \right],$$

$\lambda_N(E) = 1/\left[N_0 \sigma_{pA}^{in}(E)\right]$ is the nucleon interaction length; $x = E/E_0$ is the fraction of energy carried away by the secondary nucleon; $d\sigma_{ab}/dE$ – differential cross sections for inclusive reaction $a + A \to b + X$. The boundary conditions for Eq. (1) are $N^{\pm}(E,0) = p_0(E) \pm n_0(E)$.

Assume the solution of the system is

$$N^{\pm}(E,h) = N^{\pm}(E,0) \exp\left[-\frac{h(1 - \mathscr{Z}_{NN}^{\pm}(E,h))}{\lambda_N(E)} \right], \quad (2)$$

where $\mathscr{Z}^{\pm}_{NN}(E,h)$ are unknown functions. Substituting Eq. (2) into Eq. (1) we find the equation for these functions $\mathscr{Z}^{\pm}_{NN}$ ($\mathscr{Z}$-factors):

$$\frac{\partial(h\mathscr{Z}^{\pm}_{NN})}{\partial h} = \int_0^1 \Phi^{\pm}_{NN}(E,x)\eta^{\pm}_{NN}(E,x)\times \\ \times \exp\left[-t\mathscr{D}^{\pm}_{NN}(E,x,t)\right]dx, \quad (3)$$

where $\eta^{\pm}_{NN}(E,x) = x^{-2}N^{\pm}(E/x,0)/N^{\pm}(E,0)$,

$$\mathscr{D}^{\pm}_{NN}(E,x,h) = \frac{1-\mathscr{Z}^{\pm}_{NN}(E/x,h)}{\lambda_N(E/x)} - \frac{1-\mathscr{Z}^{\pm}_{NN}(E,h)}{\lambda_N(E)}. \quad (4)$$

By integrating Eq. (3) we obtain the nonlinear integral equation

$$\mathscr{Z}^{\pm}_{NN}(E,h) = \frac{1}{h}\int_0^h dt\int_0^1 dx\Phi^{\pm}_{NN}(E,x)\eta^{\pm}_{NN}(E,x)\times \\ \times \exp\left[-t\mathscr{D}^{\pm}_{NN}(E,x,t)\right], \quad (5)$$

which can be solved by iterations. The simple choice of zero-order approximation is $\mathscr{Z}^{\pm(0)}_{NN}(E,h) = 0$, that is $\mathscr{D}^{\pm(0)}_{NN}(E,x,h) = 1/\lambda_N(E/x) - 1/\lambda_N(E)$. For the n-th step we find

$$\mathscr{Z}^{\pm(n)}_{NN}(E,h) = \frac{1}{h}\int_0^h dt\int_0^1 dx\Phi^{\pm}_{NN}(E,x)\eta^{\pm}_{NN}(E,x)\times \quad (6) \\ \times \exp\left[-t\mathscr{D}^{\pm(n-1)}_{NN}(E,x,t)\right],$$

$$\mathscr{D}^{\pm(n)}_{NN}(E,x,h) = \quad (7) \\ \frac{1-\mathscr{Z}^{\pm(n)}_{NN}(E/x,h)}{\lambda_N(E/x)} - \frac{1-\mathscr{Z}^{\pm(n)}_{NN}(E,h)}{\lambda_N(E)}.$$

3 Simple model of the nucleon cascade

Consider a simple nucleon cascade model to illustrate the method: i) the power law PCR spectrum, $N^{\pm}(E,h=0) = N_0E^{-(\gamma+1)}$; in this case $\eta^{\pm}_{NN}(E,x) = x^{\gamma-1}$ (see Eq. (3)); ii) the total inelastic nucleonnucleus interaction cross section increases logarithmically with energy:

$$\sigma^{\rm in}_{NA}(E) = \sigma^0_{NA}[1+\beta_N\ln(E/E_1)],$$

where $\sigma^0_{NA} = 275$, $\beta_N = 0.07$, $E_1 = 100$), i.e. the nucleon mean free path decreases with energy, $\lambda_N(E) = \lambda^0_N/[1+\beta_N\ln(E/E_1)]$; ii) the nucleon production cross sections are quasiscaling ones (weak violation of the Feynman scaling), $\Phi^{\pm}_{NN}(E,x) = (\lambda_N(E)/\lambda^0_N)w^{\pm}_{NN}(x)$.

Then, in the zeroth approximation, $\mathscr{Z}^{\pm(0)}_{NN}(E,t) = 0$, we derive from Eq. 4 the function $\mathscr{D}^{\pm}$ independent of E and h:

$$\mathscr{D}^{\pm(0)}_{NN}(x) = \frac{1}{\lambda_N(E/x)} - \frac{1}{\lambda_N(E)} = -\frac{\beta_N}{\lambda^0_N}\ln x, \quad (8)$$

and Eq. 5 for the function $\mathscr{Z}_{NN}$ in the first approximation,

$$\mathscr{Z}^{\pm(1)}_{NN}(E,h) = \frac{\lambda_N(E)}{h\lambda^0_N}\int_0^h dt\times \quad (9) \\ \times\int_0^1 dxw^{\pm}_{NN}(x)x^{\gamma-1}\exp\left(t\frac{\beta_N}{\lambda^0_N}\ln x\right),$$

or

$$\mathscr{Z}^{\pm(1)}_{NN}(E,h) = \frac{\lambda_N(E)}{h\lambda^0_N}\int_0^h dt\int_0^1 dxw^{\pm}_{NN}(x)x^{\tilde{\gamma}(t)-1}, \quad (10)$$

where $\tilde{\gamma}(t) = \gamma+\beta_N(t/\lambda^0_N)$. Thus, the logarithmic growth of the inelastic nucleonnucleus interaction cross section results in the spectral index change for the secondary cosmic rays (a deviation from γ) with the atmospheric depth.

Expanding the exponent of Eq.(9) in power series for small depths and neglecting terms above the third oder, one can obtain

$$\mathscr{Z}^{\pm(1)}_{NN}(E,h) \approx \frac{\lambda_N(E)}{\lambda^0_N}\left[z^{\pm}_{NN}(\gamma) - \frac{\beta_N h}{2\lambda^0_N}\zeta^{\pm}_{NN}(\gamma)\right], \quad (11)$$

where $z^{\pm}_{NN} \equiv < x^{\gamma-1} >$ and $\zeta^{\pm}_{NN} \equiv < x^{\gamma-1}(-\ln x) >$ are the moment and the logarithmic moment of the inclusive distribution $w^{\pm}_{NN}(x)$, respectively:

$$z^{\pm}_{NN}(\gamma) = \int_0^1 dxw^{\pm}_{NN}(x)x^{\gamma-1}, \quad (12)$$

$$\zeta^{\pm}_{NN}(\gamma) = \int_0^1 dxw^{\pm}_{NN}(x)x^{\gamma-1}(-\ln x). \quad (13)$$

Thus, the first approximation of this model leads to the nucleon spectrum

$$N^{\pm}(E,h) = N_0E^{-(\gamma+1)}\exp\left[-\frac{h(1-\mathscr{Z}^{\pm(1)}_{NN})}{\lambda_N(E)}\right]. \quad (14)$$

Using estimates [9] of the momentum $< x^{\gamma-1} >$ and the logarithmic momentum, one can obtain approximately:

$$\mathscr{Z}^{\pm(1)}_{NN}(E,h) \approx \frac{\lambda_N(E)}{\lambda^0_N}z^{\pm}_{NN}[1-h/(44\lambda^0_N)]. \quad (15)$$

Thus, in the case of logarithmic rise of the inelastic nucleon–nucleus cross section $\sigma^{\rm in}_{NA}(E)$, $\mathscr{Z}^{\pm}$-factor depends on two variables, E and h. For depths $h \ll (2\lambda^0_N/\beta_N)(z^{\pm}_{NN}/\zeta^{\pm}_{NN})$ (i.e. $h \ll 44\lambda^0_N$), the h-dependence of the $\mathscr{Z}$ may be neglected:

$$\mathscr{Z}^{\pm(1)}_{NN}(E) \approx \frac{\lambda_N(E)}{\lambda^0_N}z^{\pm}_{NN}, \quad (16)$$

$$N^{\pm}(E,h) \approx N_0E^{-(\gamma+1)}\exp\left[-h\left(\frac{1}{\lambda_N(E)} - \frac{z^{\pm}_{NN}(\gamma)}{\lambda^0_N}\right)\right]. \quad (17)$$

In addition, if the nucleon interaction length is constant, then the solution of the model is exact one:

$$N^{\pm}(E,h) = N_0E^{-(\gamma+1)}\exp\left[-\frac{h(1-z^{\pm}_{NN}(\gamma))}{\lambda^0_N}\right]. \quad (18)$$

This can be seen from Eq. (9), where we have now to put $\beta_N = 0$. Hence the exact solution $\mathscr{Z}^{\pm}_{NN} = z^{\pm}_{NN}(\gamma)$ immediately follows.

4 Muon fluxes in the atmosphere

As the major sources of the atmospheric muons we consider two-particle leptonic decays $\pi_{\mu 2}$ and $K_{\mu 2}$ decays, three-particle semileptonic decays, $K^{\pm}_{\mu 3}$, $K^{0}_{\mu 3}$ and small contribution originated from decay chains $K \to \pi \to \mu$ ($K^0_S \to \pi^+\pi^-$, $K^{\pm} \to \pi^{\pm}\pi^0$). More details concerning the meson cascade treatment can be found in Ref.[6].

As the primary cosmic ray spectra and composition in wide energy range folowing models are used: 1) the model by Zatsepin & Sokolskaya (ZS) [10], and 2) the recent cosmic ray spectrum approximation by Gaisser [11, 12] (we use the version for the mixed CR population 3: Hillas, Gaisser in Fig. 1 and HGm in Fig. 2). The model by Zatsepin and Sokolskaya describes well data of the ATIC2 direct measurements [13, 14] in the range $10 - 10^5$ GeV and gives a motivated extrapolation of these data up to 100 PeV – the energy region for which the cosmic ray spectrum and composition is reconstructed based on the measured characteristics of EAS. The ZS proton spectrum at $E \gtrsim 10^6$ GeV is compatible with KASCADE data [15] as well the helium one within the range of the KASCADE spectrum obtained with the usage of hadronic models QGSJET01 and SIBYLL, and well agree with the HGm up to 10 PeV.

The high energy spectra of the conventional and prompt muons at ground level calculated for the vertical direction are shown in Fig. 2 together with the experimental data. The inclined shaded bands here indicate the conventional muon flux calculated with KM model for the case of the ATIC-2 primary spectrum (narrow cyan band) and the GAMMA one (green band). The width of the bands corresponds to statistical errors in the ATIC-2 and GAMMA experiments. Solid lines indicate the calculations with use of ZS spectrum and hadronic models KM (black), QGSJET II-03 (blue), dashed, dash-dotted - SIBYLL 2.1. The red line and bold dotted show the flux calculated with HGm spectum for QGSJET II-03 and SIBYLL 2.1 respectively. In the computation with QGSJET II-03, we rescale the muon flux by factor 1.2 to take into account results obtained with renewed version QGSJET II-04 [16] (see also [17]) . The experimental data comprise the measurements of L3+Cosmic as well as the data (converted to the surface) of deep underground experiments MSU, MACRO, LVD, Frejus, Baksan, Artyomovsk (see the references in

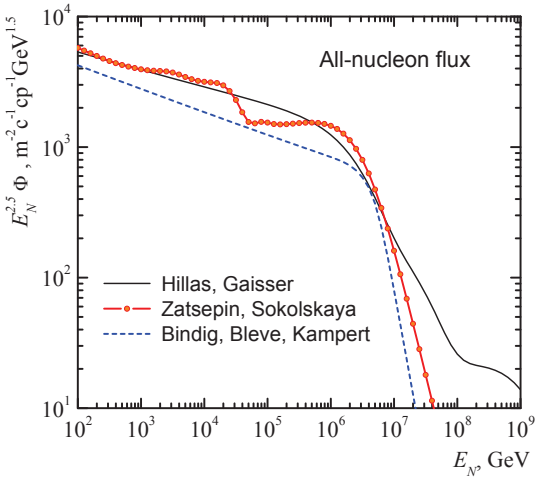

Figure 1: All-nucleon CR spectrum: three parameterisations.

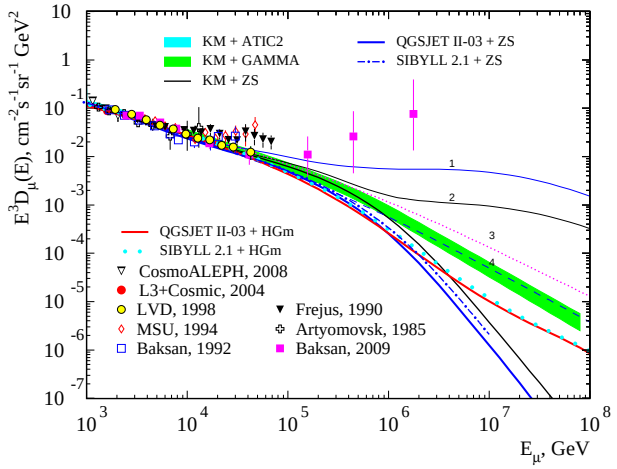

Figure 2: Conventional and prompt muon fluxes close to vertical.

[6]). Notice that the calculation results do not fit well the Frejus and MSU data even if the prompt muon component is taken into account (thin lines 1,2 in Fig. 2), while the LVD data are well described.

The ZS model seems to be a reasonable bridge from TeV energy range to PeV one (solid line), providing a junction of the "low" and high energy ranges. However, above 10^6 GeV the muon flux is apparently affected by the primary cosmic ray ambiguity in the vicinity of 'knee'. To illustrate this we plot also our early predictions [18, 19, 20] for the conventional muon flux made with primary cosmic ray spectra by Nikolsky, Stamenov, and Ushev (NSU)[21] (dotted line 3) as well as by Erlykin, Krutikova, and Shabelsky (EKS) [22] (dashed line 4). The index γ of the NSU primary nucleons is 1.62 and 2.02 before and beyond the "knee" ($\sim$ 3 PeV) correspondingly, while $\gamma = 1.7$ and 2.1 for the EKS spectrum.

The prompt muon contribution due to decays of charmed hadrons at high energies is shown for the recombination quark-parton model [18, 23] (RQPM, line 1 in Fig. 2), and the quark-gluon string model (QGSM, line 2) [24, 23] . These clculations were peformed with NSU primary spectrum, therefore they can serve here as upper limits for the prompt neutrino flux due to RQPM or QGSM since we ignore here the differences in prompt muon flux calculations related both to atmospheric hadron cascade features and the primary cosmic ray spectrum and composition (see discussion in Ref. [12]).

The difference of the muon flux predictions resulted from that of the primary cosmic ray spectra becomes apparent at high energy: the flux obtained with QGSJET-II for ZS spectrum at 2 PeV is less by a third of the flux for HGm spectrum.

Figure 2 also shows the muon energy spectrum in the range from 3 TeV to 2 PeV reconstructed by the method of multiple interactions from the Baksan Underground Scintillation Telescope (BUST) data [25]. The results are compared with the previous BUST measurements and the data of other experiments as well as with the calculations for various models of the muon spectrum. The muons with energies above 100 TeV are of particular interest. The knee in the PCR spectrum of an astrophysical origin affects the muon spectrum in quite a definite way: the muons inherit the PCR spectral index ($\gamma \approx 2.7$) at comparatively low en-

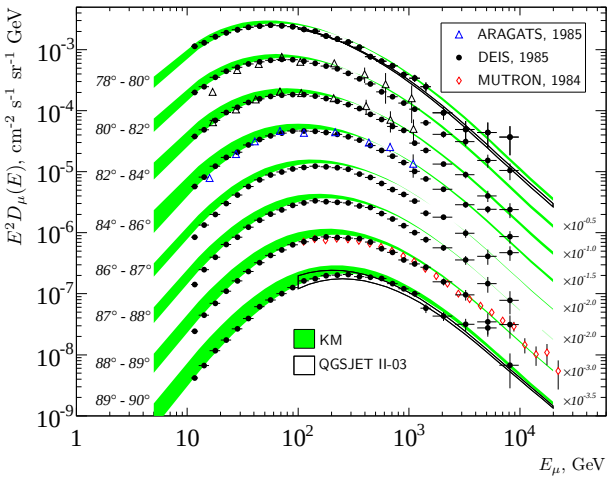

Figure 3: Energy spectra of muons near the horizontal direction at sea level. The dots show the ARAGATS [27], DEIS [28], and MUTRON [29] experimental data. The shaded and hatched areas indicate our calculations for the ATIC-2 primary spectrum using the KM and QGSJET-II-03 interaction models.

ergies (below 1 TeV), while at higher energies the muon spectrum index is close to 3.7. In contrast, in the case of a constant slope of the PCR spectrum, the knee effect in EASs could be produced by high energy muons and neutrinos carrying away the required energy. These muons, whose appearance is expected at energies near 100 TeV, could be produced through some new physical processes. As the energy increases, the contribution from this component rises more rapidly than the flux of muons from the decays of charmed particles, thus ensuring the anomalous muons identification. However, the corresponding anomalous neutrino flux was not detected with the IceCube neutrino telescope [26].

Figure 3 shows the calculated differential energy spectra of muons near the horizontal direction and the measurements of ARAGATS EAS array [27], DEIS [28], and MUTRON [29] magnetic spectrometers for zenith angles $78-90^\circ$. Shaded areas indicate the calculation with the KM hadronic model, while the hatched areas correspond to the calculation with the QGSJET-II-03 model. The predictions of the QGSJET-II model are shown only for two ranges of angles, $78^\circ - 80^\circ$ and $89^\circ - 90^\circ$. The QGSJET-II model describes well the data of the muon experiments at large zenith angles.

Acknowledgments

We acknowledge the support of the Russian Federation Ministry of Education and Science, agreement N 14.B37.21.0785.

References

[1] S. Sinegovsky, O. Petrova and T. Sinegovskaya, Proc. 32nd ICRC, Beijing, 2011, V.4, p. 291; arXiv: 1109.3576v1 [astro-ph.HE].
[2] O. N. Petrova, T. S. Sinegovskaya, S. I. Sinegovsky, Phys. Part. Nucl. Lett. 9 (2012) 766-768.
[3] S. Ostapchenko, Nucl. Phys. B (Proc. Suppl.) 151 (2006) 143-146; Nucl. Phys. B (Proc. Suppl.) 175-176 (2008) 73-80; Phys. Rev. D 74 (2006) 014026.
[4] R.S. Fletcher et al. Phys. Rev. D 50 (1994) 5710; E.-J. Ahn et al. Phys. Rev. D 80 (2009) 094003.
[5] L. R. Kimel, N. V. Mokhov, Izv. Vyssh. Uchebn. Zaved., Fiz. 10, 17 (1974). A. N. Kalinovskii, N. V. Mokhov, and Yu. P. Nikitin, Passage of High Energy Particles through Matter, AIP, New York, 1989.
[6] A.A. Kochanov, T.S. Sinegovskaya, S.I. Sinegovsky, Astropart. Phys. 30 (2008) 219-233.
[7] A. A. Kochanov, T. S. Sinegovskaya, S. I. Sinegovsky, J. Exp. Theor. Phys. 116 (2013) 395-413.
[8] V. A. Naumov, T. S. Sinegovskaya, Phys. Atom. Nucl. 63 (2000) 1927-1935; hep-ph/0106015.
[9] A. N. Vall, V. A. Naumov, S. I. Sinegovskii, Sov. J. Nucl. Phys. 44 (1986) 806-812.
[10] V.I. Zatsepin, N.V. Sokolskaya, Astronomy & Astrophys. 458 (2006) 1-5.
[11] T. Gaisser, Astropart. Phys. 24 (2012) 801-806.
[12] T. Gaisser, arXiv:1303.1431v1 [hep-ph].
[13] A. D. Panov et al., Bull.Russ. Acad. Sci.Phys. 71 (2007) 494-497.
[14] A. D. Panov et al., Bull. Russ. Acad. Sci. Phys. 73 (2009) 564-567.
[15] T. Antoni et al., Astropart. Phys. 24 (2005) 1-25.
[16] S. Ostapchenko, Phys. Rev. D 83 (2011) 014018.
[17] T. Pierog, J. Phys. Conf. Ser. 409 (2013) 012008.
[18] E.V. Bugaev et al. Phys. Rev. D 58 (1998) 054001; hep-ph/9803488.
[19] T. S. Sinegovskaya, S. I. Sinegovsky, *Phys. Rev. D* **63**, 096004 (2001).
[20] A. A. Kochanov, T. S. Sinegovskaya, S. I. Sinegovsky, Phys. Atom. Nucl. 70 (2007) 1913-1925.
[21] S.I. Nikolsky, I.N. Stamenov, S.Z. Ushev, Sov. Phys. JETP 60 (1984) 10-21.
[22] A. D. Erlykin, N. P. Krutikova, and Yu. M. Shabelskii, Yad. Fiz. 45, 1075 (1987).
[23] E.V. Bugaev et al. Nuovo Cim. C 12 (1989) 41-73.
[24] A. B. Kaidalov and O. I. Piskunova, Sov. J. Nucl. Phys. 41 (1985) 816.
[25] A. G. Bogdanov et al. Astropart. Phys. 36 (2012) 224236.
[26] R. Abbasi et al. (IceCube Collaboration), Phys. Rev. D 83 (2011) 012001.
[27] T.L. Asatiani et al., Izv. Akad. Nauk SSSR, Ser. Fiz. 49 (1985) 1377.
[28] O.C. Allkofer et al., Nucl. Phys. B 259 (1985) 1.
[29] S. Matsuno et al., Phys. Rev. D: Part. Fields 29 (1984) 1.